Research Article

Ultrathin Zn-Gallate Catalyst: A Remarkable Performer in CO_2 and Propylene Oxide Polymerization

Yongmoon Yang,[#] Kihyuk Sung,[#] Jong Doo Lee, Junho Ha, Heeyoun Kim, Jinsu Baek, Jeong Hwa Seo, Seung-Joo Kim,[*] Bun Yeoul Lee, Seung Uk Son, Byeong-Su Kim, Yongsun Kim, Ji-Yong Park, and Hye-Young Jang[*]

Cite This: https://doi.org/10.1021/acssuschemeng.3c06058

Read Online

ACCESS | Metrics & More | Article Recommendations | SI Supporting Information

ABSTRACT: Zn-gallate, an innovative catalyst synthesized using cost-effective zinc salts and gallic acid without complicated synthetic procedures, has been successfully applied in the copolymerization of CO_2 and propylene oxide. Zn-gallate displays exceptionally thin sheets with a thickness of 1−2 nm, leading to remarkable catalytic activity, high carbonate linkage proportion, and minimal monomer formation (3.01 kg/g-cat, f_{CO_2} = 0.97, and selectivity 91%). Zn-gallate outperforms other heterogeneous catalysts for the polymerization of CO_2 and propylene oxide.

remarkable polymerization activity: 3.01 kg/g-cat, f_{CO_2} 0.97, polymer selectivity 91% cost-effective and easy catalyst preparation using nature-abundant gallic acid

Furthermore, the polycarbonates synthesized using Zn-gallate exhibit substantially high molecular weights. A comprehensive characterization of Zn-gallate has been undertaken, employing SEM, TEM, BET, AFM, PXRD, IR, CP-TOSS ^{13}C NMR, XPS, TGA, and ICP analyses, which provided valuable insights into the exceptional catalytic properties of this novel catalyst.

KEYWORDS: CO_2 utilization, Zn-gallate, polypropylene carbonate, CO_2 polymer, ultrathin catalyst

INTRODUCTION

Anthropogenic carbon emissions are causing climate change, necessitating a shift from fossil fuels in society and industry to prevent a global catastrophe. In 2021, the annual rate of CO_2 emissions was 52.8 Gt.[1,2] To restrict the rise in global temperature to 2 °C, emissions need to remain below 17 Gt per year by 2030.[2] This appears to be a challenging task given the current high rate of annual emissions and the limited use of industrial CO_2.[3,4] To address this challenge, developing new technologies that can convert large amounts of CO_2 into commercially valuable products is vital.[5,6] Substituting fossil-fuel-based processes with sustainable CO_2-utilizing processes can play an important role in achieving carbon neutrality in time.

Leveraging CO_2 as a carbon source in polymerization holds great potential for advancing sustainable chemical processes because this approach broadens the spectrum of plastic products that can incorporate carbon dioxide. Polymers that are synthesized from CO_2 and epoxides are important as they contain a substantial amount of CO_2 in their polycarbonate chains. In addition, these polymers have diverse commercial uses, including coatings, adhesives, and polyurethane formulations.[7−9] Due to their high CO_2 content and versatile applications in final products, significant efforts have been directed toward the development of effective catalysts. In 1969, Inoue reported the first zinc-based polymerization catalyst derived from diethyl zinc and water, exhibiting the catalytic

activity of 0.013 kg/g-cat.[10] Subsequently, there has been extensive research on both homogeneous and heterogeneous zinc-based catalysts to enhance catalytic activity, increase the carbonate fraction, and decrease monomer carbonate formation.[11−20] While heterogeneous catalysts offer economic advantages, the lack of understanding of their catalytic activity impeded the advancement of efficient zinc-based heterogeneous catalysts. Currently, the most potent heterogeneous catalyst reported for producing alternating polycarbonate from propylene oxide (PO) and CO_2 is zinc glutarate (ZnGA), which exhibited an activity of 0.083 kg/g-cat.[15,20−22] However, the catalytic activity of ZnGA is still low to be used in the commercial polymerization process although extensive studies have attempted to improve ZnGA's catalytic activity.[23−29]

This study introduces a novel approach to address the limited catalytic activity observed in zinc-based heterogeneous catalysts. Our proposal involves the utilization of an ultrathin zinc catalyst, wherein the abundant active sites of thin sheets are exposed to CO_2 and epoxides, resulting in high catalytic activities for polymerization (Figure 1). It has been observed
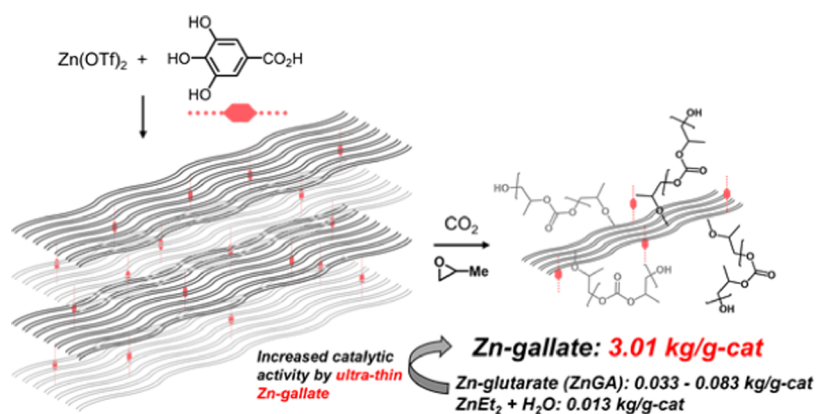
Figure 1. Formation of ultrathin Zn-gallate and its polymerization.

that when zinc salts and gallic acid react, they form a layered structure in which gallic acid is intercalated between zinc hydroxide layers.[30−38] In this study, we synthesized Zn-gallate using $Zn(OTf)_2$ (OTf = trifluoromethanesulfonate) and gallic acid,[39] and interestingly, this compound exhibited exceptionally thin sheets with a thickness (1−2 nm). We employed this ultrathin catalyst for the copolymerization of CO_2 and epoxide, and it exhibits outstanding catalytic activity (3.01 kg/g-cat), a high proportion of carbonate linkages (f_{CO_2} = 0.97), and limited monomer formation (9%). For comparison, the catalytic activities of ZnGA, synthesized from ZnO and glutaric acid, and $Zn(OAc)_2 \cdot 2H_2O$, glutaric acid, and PE6400, were reported to be 0.033 and 0.083 kg/g-cat, respectively.[21,29] To shed light on its exceptional catalytic properties, we provide a comprehensive analysis of the morphology and composition of Zn-gallate.

EXPERIMENTAL SECTION

General. PO was dried by stirring over CaH_2 and then vacuum-transferred to a storage vessel. PO was transferred to an autoclave within a glovebox, and the subsequent polymerization reactions and the entire workup were conducted in the well-ventilated fume hood. ZnGA and DMC (Table 2) were prepared according to the published procedure.[21,40]

Procedure for the Preparation of Zn-gallate 1. Gallic acid (114 mg, 0.670 mmol) and zinc trifluoromethanesulfonate (487 mg, 1.34 mmol) were dissolved in anhydrous methanol (5.0 mL). While vigorously stirring the mixture, a 3% aqueous solution of NH_4OH (3%) was gradually introduced until the pH reached 10. The resulting slurry was subjected to centrifugation and washed with methanol until the pH reached 7. The resulting gray solid product was then dried under reduced pressure at room temperature for a duration of 1 day, yielding 386 mg of product.
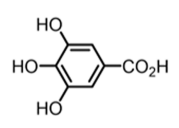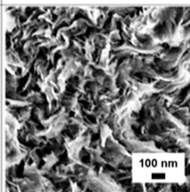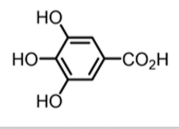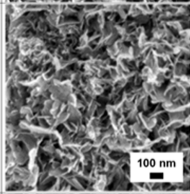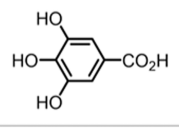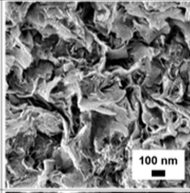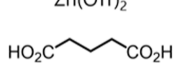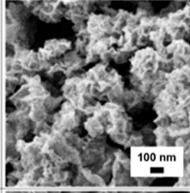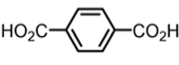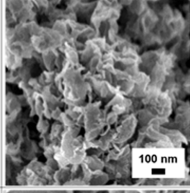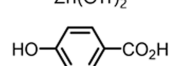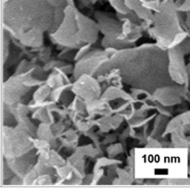
General Procedure for the Polymerization. In a controlled atmosphere glovebox, a 50 mL autoclave was loaded with the catalyst (4.4 mg) and propylene oxide (4.36 g, 75.1 mmol). The autoclave was subsequently pressurized with CO_2 and then heated to 80 °C. The autoclave was allowed to cool to room temperature after 20 h, and the CO_2 pressure was gradually released. For entries 1−5 of Table 2, reactions were conducted in a 50 mL autoclave with a cylindrical PTFE magnetic stirring bar (20 × 8 mm). The reactions of entries 6−9 (Table 2) and the reaction using 20.0 g of PO were performed in a 100 mL autoclave with an oval PTFE magnetic stirring bar (25 mm × 12 mm). All reactions were performed under 650 rpm. After the reaction, the reactor was taken off the oil bath. It took 40 min to cool down. Stirring was stopped during the cooling phase. A minor portion of the crude polymer was employed for ^1H NMR analysis. The resultant polymer was dissolved in dichloromethane and precipitated using methanol.

RESULTS AND DISCUSSION

To prepare zinc catalysts, we employed a synthetic protocol generating zinc hydroxide layers in the presence of intercalated organic compounds.[31,34,36,41−43] In this method, aqueous ammonium hydroxide (NH_4OH) was a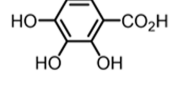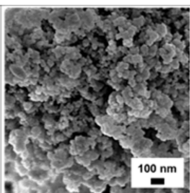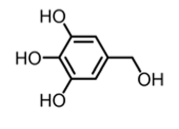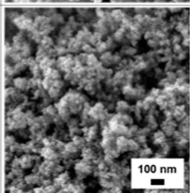dded to a mixture of zinc(II) salts and organic compounds in MeOH (Table 1). By utilizing suitable organic compounds, we aimed to manipulate the morphology of the zinc catalysts. The functional groups present in the intercalating compounds could potentially influence the binding affinity to the layers, allowing for modulation. The field emission scanning electron microscopy (FE-SEM) images of zinc catalysts obtained from various zinc salts and organic compounds displayed diverse morphologies (Table 1). The SEM images of Zn catalysts involving gallic acid (Zn-gallates **1−3**) revealed a bundle of wrinkled sheets. This morphological characteristic was observed in the previous report on ZnGA exhibiting enhanced catalytic activity in polycarbonate synthesis.[21] Conversely, zinc catalysts using glutaric acid, terephthalic acid, 4-hydroxy benzoic acid, 2,3,4-trihydroxy benzoic acid, and 5-(hydroxymethyl)benzene-1,2,3-triol exhibited different morphologies, such as aggregated grains, flakes, and wrinkled particles (Table 1). Subsequently, these catalysts were then subjected to polymerization conditions using PO and CO_2 (Table 1). The mixture of PO (75 mmol) and the catalyst (4.4 mg) was pressurized with CO_2 (40 bar) and heated at 80 °C for 20 h. The zinc catalysts (Zn-gallates **1**, **2**, and **3**) derived from gallic acid exhibiting wrinkled bundle morphology demonstrated higher catalytic activities than other catalysts (990, 569, and 721 g/g-cat, respectively). The zinc catalysts involving dicarboxylic acids like glutaric acid and terephthalic acid demonstrated catalytic activities of 12 g/g-cat and 3.3, respectively. Zinc catalysts containing 4-hydroxy benzoic acid, 2,3,4-trihydroxy benzoic acid, and 5-(hydroxymethyl)benzene-1,2,3-triol, which share structural similarity with gallic acid, showed no significant catalytic activities. The zinc catalyst synthesized without an organic intercalating agent exhibited low catalytic activity (3.2 g/g-cat). Overall, the presence and positioning of functional groups in the organic compounds play a crucial role in the catalytic activity and the morphology of zinc catalysts.

More information regarding the polymerization catalyzed by Zn-gallate **1** can be found in Table 2. The optimal ratio of $Zn(OTf)_2$ and gallic acid for the synthesis of Zn-gallate **1** was determined to be 2:1, resulting in the highest catalytic activity among the tested catalyst compositions (see Supporting Information, Table S1). Zn-gallate **1** demonstrated a high

Table 1. List of Zinc Catalysts and Their Catalytic Activities for the Polymerization of PO and CO_2

catalyst	reactants	SEM image	catalytic activity
Zn-gallate **1**	Zn(OTf)$_2$ HO—(gallic acid: trihydroxybenzene)—CO$_2$H	100 nm	990 g/g-cat
Zn-gallate **2**	ZnCl$_2$ HO—(gallic acid)—CO$_2$H	100 nm	569 g/g-cat
Zn-gallate **3**	Zn(NO$_3$)$_2$ HO—(gallic acid)—CO$_2$H	100 nm	721 g/g-cat
Zn-glu	Zn(OTf)$_2$ HO$_2$C—CO$_2$H	100 nm	12 g/g-cat
Zn-tereph	Zn(OTf)$_2$ HO$_2$C—(benzene)—CO$_2$H	100 nm	3.3 g/g-cat
Zn-Hben	Zn(OTf)$_2$ HO—(benzene)—CO$_2$H	100 nm	6.3 g/g-cat
Zn-triHben	Zn(OTf)$_2$ HO—(benzene)—CO$_2$H, HO, OH	100 nm	9.8 g/g-cat
Zn-triHalc	Zn(OTf)$_2$ HO—(benzene)—OH, HO	100 nm	9.0 g/g-cat

carbonate linkage (f_{CO_2} = 0.97) and effectively suppressed the formation of monomer carbonate (selectivity = 98%) (entry 1 of Table 2). The utilization of undistilled PO resulted in a slightly lower catalytic activity (752 g/g-cat) than the reaction

using distilled PO (entry 1 of Table 2), suggesting that the presence of water affects the catalyst's performance. To figure out the chain end group, the matrix-assisted laser desorption/ionization-time-of-flight (MALDI-ToF) analysis of polycarbonates obtained during a shorter period of reaction time (3 h) was attempted. The observed major signal corresponded to $M_{observed}$ (Da) = $n \times$ (PO−CO_2) + PO + H_2O + Na$^+$ (see Supporting Information, Figure S1).

The lower pressure of CO_2 and lower temperatures resulted in lower catalytic activities (entries 2−4). Employing the higher temperature (90 °C) provided more products (entry 5). Reducing the amount of catalyst to 0.5 and 0.34 mg of catalyst per g-PO led to enhanced catalytic activities of 1470 and 1414 g/g-cat, respectively (entries 6 and 8). Furthermore, extending the reaction time facilitated polymer formation, achieving the highest activity of 3014 g/g-cat (entry 9). Polymers exhibiting elevated catalytic activities demonstrated high molecular weights. This characterization was accomplished using size-exclusion chromatography with multiangle light scattering (SEC-MALS) in THF. The additional analysis of the polymer's molecular weights was conducted using size-exclusion chromatography in DMF (see Supporting Information, Table S2). Analysis of the polymer's ^{13}C NMR spectrum revealed a predominance of head-to-tail linkage (72%) (see Supporting Information, Figure S2) The large-scale polymerization was conducted with 20.0 g of PO under the conditions specified in entry 6 (Table 2), exhibiting a catalytic activity of 1349 g/g-cat, f_{CO_2} of 0.96, and a selectivity of 98% (see Supporting Information, Scheme S1). Furthermore, Zn-gallate **1** exhibited superior catalytic activities compared to other heterogeneous catalysts. The use of ZnGA resulted in a significantly lower catalytic activity (entry 10 of Tables 2 and S5). Double metal cyanide (DMC) derived from ZnCl$_2$, K$_3$Co(CN)$_6$, and ^{t}BuOH facilitated polymerization, exhibiting lower catalytic activities and much lower f_{CO_2} (entry 11).

To elucidate the high catalytic activity of Zn-gallate **1**, we investigated its physical and chemical properties. The morphology of Zn-gallate **1**, illustrated in Figure 2a−c, reveals ultrathin sheets with thicknesses ranging from 1 to 2 nm by FE-SEM and transmission electron microscopy (TEM). In contrast to the previous LZH forming methods,[36] our synthetic approach yielded a weakly bound layered structure composed of ultrathin sheets. The Zn-gallate **1**'s loosely layered structure was further confirmed by analyzing N$_2$ adsorption−desorption isotherm curves using the Brunauer−Emmett−Teller (BET) theory (Figure 2d,e). The surface area of Zn-gallate **1** was found to be 157 m^2/g, and the total pore volume was 0.27 cm^3/g. To assess the disintegration of the loosely layered structure in solution, we deposited dilute colloidal dispersions of Zn-gallate **1** in EtOH onto silicon wafers using the spin-coating technique and examined them using atomic force microscopy (AFM) (Figure 2f). The height profile revealed the disintegration of the layered structure into ultrathin sheets with a thickness of 1−1.5 nm (Figure 2g). The Tyndall scattering photo confirmed the colloidal dispersion of Zn-gallate **1** (Figure 2h). These characteristics contribute to the outstanding catalytic performance of Zn-gallate **1** in polymerization reactions.[27]

The chemical structure of Zn-gallate **1** was characterized using powder X-ray diffraction (PXRD), inductively coupled plasma-atomic emission spectroscopy (ICP-AES), infrared absorption (IR), solid-state CP-TOSS ^{13}C nuclear magnetic

Table 2. Zn-Gallate-Catalyzed Polymerization of Propylene Oxide (PO) and CO_2[a]
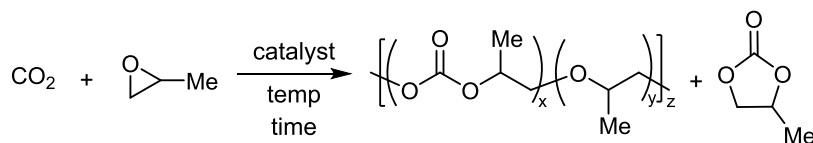
| entry	catalyst (mg/g-PO)	CO_2 (bar)	temp	time	activity (g/g-cat)	f_{CO_2}[c]	selec.[c]	M_n[d]	M_w/M_n[d]	T_g (°C)
1	Zn-gallate **1** (1.0)	40	80 °C	20 h	990	0.97	98%	367k	3.1	39
2	Zn-gallate **1** (1.0)	30	80 °C	20 h	615	0.97	98%	151k	7.6	39
3	Zn-gallate **1** (1.0)	40	70 °C	20 h	510	0.98	98%	169k	6.8	39
4	Zn-gallate **1** (1.0)	40	25 °C	240 h	256	0.98	93%	86k	5.3	36
5	Zn-gallate **1** (1.0)	40	90 °C	20 h	1190	0.97	92%	501k	2.5	39
6	Zn-gallate **1** (0.5)	40	80 °C	20 h	1470	0.97	95%	1610k	1.9	40
7	Zn-gallate **1** (0.5)	40	90 °C	20 h	1430	0.96	93%	340k	2.6	39
8	Zn-gallate **1** (0.34)	40	80 °C	20 h	1414	0.98	98%	625k	2.4	39
9	Zn-gallate **1** (0.34)	40	80 °C	72 h	3014	0.97	91%	889k	2.5	39
10	ZnGA (1.0)	40	80 °C	20 h	8.4	0.94	93%	33k[e]	10[e]	36
11[b]	DMC (1.0)	40	90 °C	20 h	1093	0.26	92%	88k	2.9	10

[a]Reaction conditions: PO (75 mmol, entries 1−5; 150 mmol, entries 6 and 7; 225 mmol, entries 8 and 9) was used. [b]The data was extracted from ref 29. [c]f_{CO_2}: {[PPC]}/{[PPC] + [PPO]} determined by ^{1}H NMR, selectivity: [PO incorporated into polymer]/{[propylene carbonate] + [PO incorporated into polymer]} determined by ^{1}H NMR. [d]M_n and M_w/M_n values were determined by SEC-MALS (THF). [e]M_n and M_w/M_n values were determined by SEC (THF).
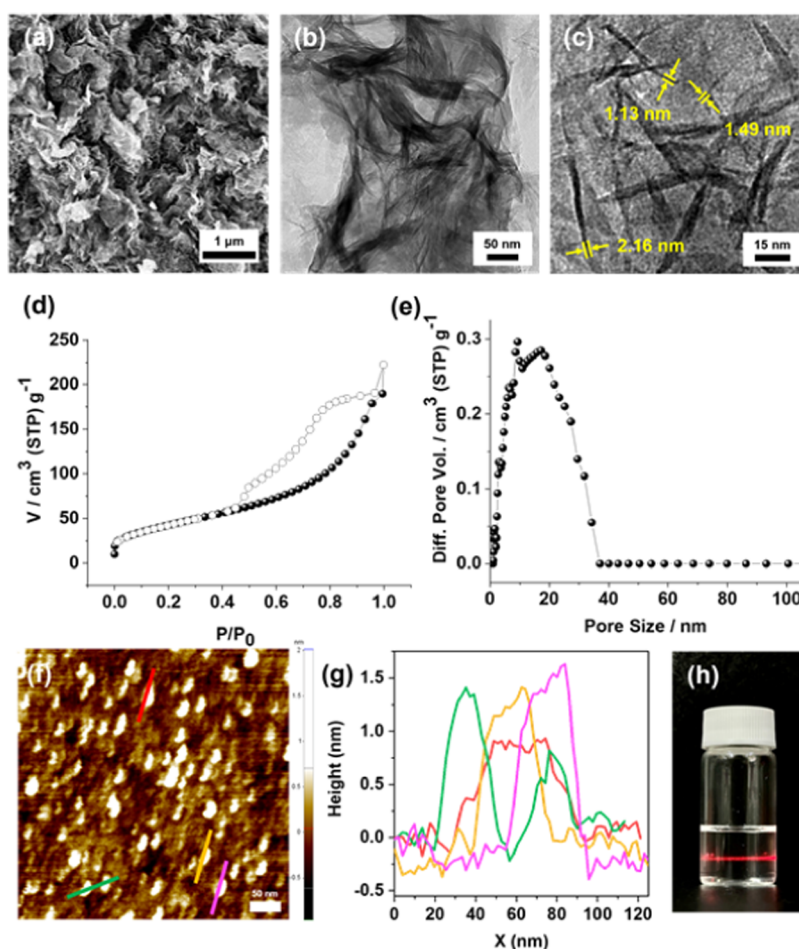
Figure 2. (a) SEM image of Zn-gallate **1**, (b) and (c) TEM images of Zn-gallate **1**, (d) N_2 absorption−desorption isotherm curves obtained at 77K, (e) pore size distribution diagram based on DFT method of Zn-gallate **1**, (f) AFM image of ultrathin sheets, (g) height profiles of ultrathin sheets, and (h) Tyndall image of Zn-gallate **1** in EtOH.

resonance (NMR) spectroscopy, thermal gravimetric analysis (TGA), and X-ray photoelectron spectroscopy (XPS). The

PXRD of Zn-gallate is depicted in Figure 3a. Despite the challenge posed by the overlap of broad peaks, several
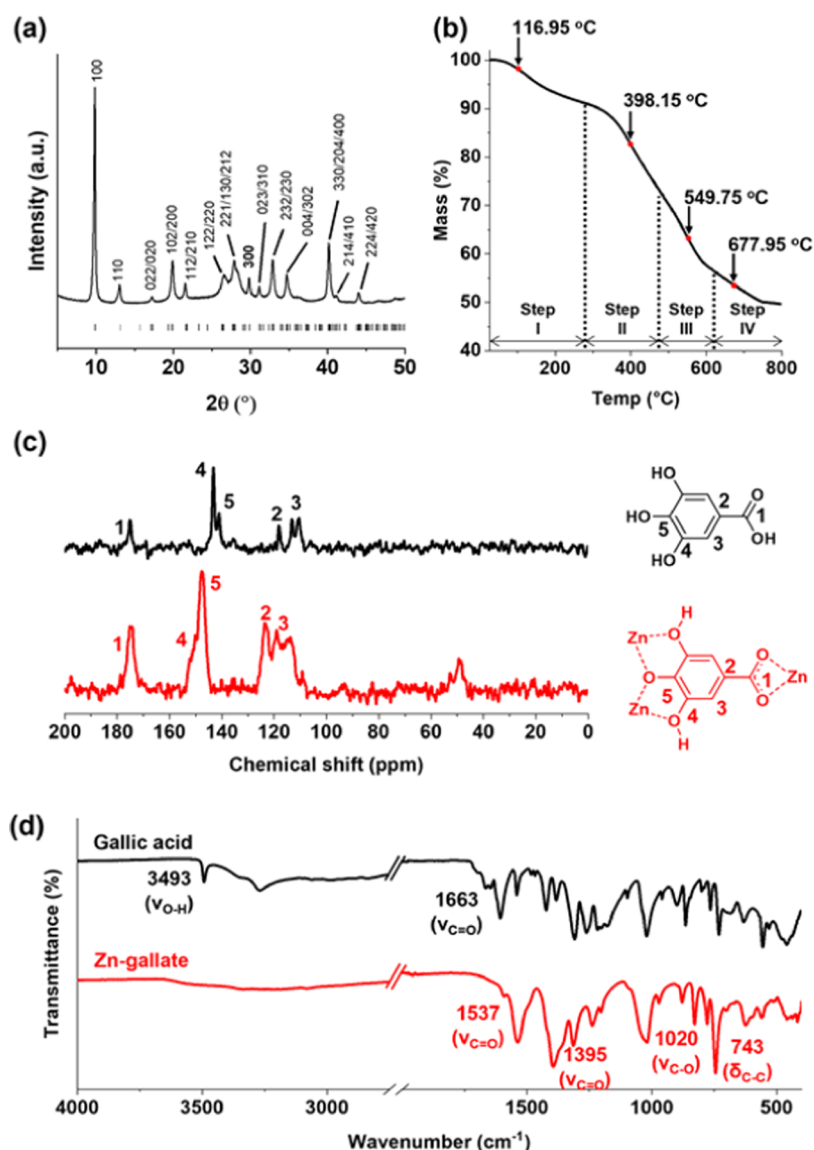
Figure 3. (a) PXRD patterns of Zn-gallate **1**, (b) the TGA curve of Zn-gallate **1**, (c) CP-TOSS ^{13}C NMR spectra of gallic acid and Zn-gallate **1**, and (d) IR spectra of gallic acid and Zn-gallate **1**.

prominent peaks were successfully indexed within an orthorhombic system defined by parameters: a = 8.97 Å, b = 10.24 Å, and c = 10.37 Å. The space group $Pbc2_1$ was selected by examining the absence of nonindexed reflections. The determination of atomic coordinates was facilitated through the direct method using EXPO2013 software.[44] While coordinates of Zn were ascertained, the low crystallinity of the sample impeded the resolution of atomic coordinates for lighter elements (O, C, and H).

Inductively coupled plasma-atomic emission spectroscopy (ICP-AES) was utilized to determine the composition of Zn-gallate **1**, and it revealed 42 wt % of Zn. The quantitative ^{1}H NMR analysis of Zn-gallate **1** in basic D_2O solution was conducted using an internal standard (isonicotinic acid), which showed 34 wt % of gallate in Zn-gallate **1** (see Supporting Information, Figures S7−S9). Based on these results, Zn-gallate **1** was concluded to have the composition of $Zn_3(OH)_4(C_7H_4O_5)\cdot1.5CH_3OH$ (where $C_7H_4O_5$ represents dianionic gallate, the theoretical value of Zn 41 wt % and gallate 35 wt %). This composition has been verified through

thermogravimetric analysis (TGA) of Zn-gallate **1** (Figure 3b). The analysis revealed four stages of mass loss, resulting in a total weight reduction of 50%. The initial weight loss is ascribed to the elimination of adsorbed water and methanol (9%), and the subsequent three losses are attributed to layer collapse and gallate decomposition, accounting for 41%.[31] The expected mass loss during the transformation from $Zn_3(OH)_4(C_7H_4O_5)\cdot1.5CH_3OH$ to 3ZnO is theoretically 49%, displaying an alignment with the observed total mass loss (50%). The solid-state CP-TOSS ^{13}C NMR spectrum of Zn-gallate **1** showed the main ^{13}C peaks at 175, 148, and 123− 114 ppm, which corresponded to the carbonyl and aromatic carbons of gallate (Figure 3c). The peak at 49 ppm was assigned to the carbon of methanol. The IR spectrum of Zn-gallate **1** revealed vibration peaks of the zinc-coordinated gallic acid moiety at 1537 and 1395 cm^{-1}, which correspond to asymmetric and symmetric C=O stretching vibration modes, respectively (Figure 3d).[32] The peaks at 1020 and 743 cm^{-1} were assigned to C−O stretching and δ_{CC} benzene ring. XPS was employed to examine the chemical environment of zinc,
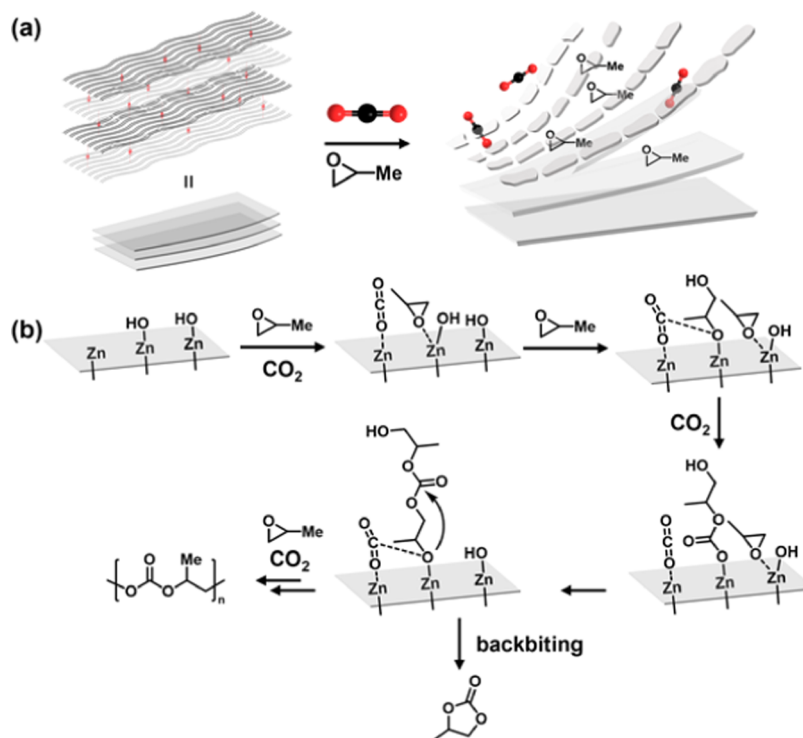
Figure 4. (a) Disintegration of Zn-gallate **1** and (b) the polymerization of CO_2 and PO at the active site.

carbon, and oxygen atoms in Zn-gallate **1** (Figure S11). The $2p_{1/2}$ and $2p_{3/2}$ orbitals of Zn displayed peaks at 1044.7 and 1021.7 eV, respectively.[36] The deconvoluted XPS of the C 1s spectrum exhibited the major bands at 284.7 and 283.3 eV assigned to C 1s of the gallic acid aromatic ring. A peak at 287.5 eV was identified as carboxylic acid. The O 1s core level spectrum demonstrated a strong peak at 531.0 eV assigned to O 1s coordinated to zinc ions, and a weak peak at 532.6 eV was assigned to oxygen atoms of carboxylic acid.

The remarkable enhancement in the catalytic activity of Zn-gallate can be ascribed to the disintegration of its layered structure during the polymerization reaction (Figure 4a).[45] This disintegration results in the creation of ultrathin Zn-gallate, generating numerous catalytically active zinc sites, including coordinatively unsaturated zinc sites and Zn−OH sites. The proposed mechanism for PPC formation is based on the catalytic action of ZnGA, with Zn−OH serving as an initiator (Figure 4b).[15] Our analysis of the polymer chain end indicates that Zn-gallate initiates the reaction through Zn−OH, which primarily activates PO, while the coordinatively unsaturated sites are responsible for activating CO_2. Initially, the epoxide coordinates with Zn−OH, facilitating the nucleophilic addition of the hydroxide group of Zn−OH. This results in the formation of zinc-alkoxides. Subsequently, the zinc alkoxide readily undergoes insertion into CO_2 at the proximal CO_2-coordinated zinc, leading to the formation of zinc−carbonates. Through a repeated addition of PO and CO_2 in an alternating manner, the synthesis of polypropylene carbonates occurs. This suppresses the undesired formation of polypropylene glycol (PPG) through the homopolymerization of PO and propylene carbonate monomers through the backbiting mechanism. It is worth noting that deviations from the optimal reaction conditions, such as variations of reaction temperatures (25 and 90 °C) and extended reaction times, result in increased backbiting and consequently elevated

propylene carbonate formation (entries 4, 5, 7, and 9 of Table 2). The competitive generation of propylene carbonate is facilitated when polymerization is inefficient due to low temperature and diminished catalytic activity. Elevated temperatures increase the formation of thermodynamic products, including propylene carbonate. The utilization of low CO_2 pressure (5 bar) exhibited lower catalytic activity (428 g/g-cat) with a diminished f_{CO_2} (0.66), while maintaining a 96% selectivity for polymer formation over monomer carbonate (see Supporting Information, Scheme S2). This can be attributed to the decreased CO_2-coordinated zinc sites, promoting homopolymerization of PO.

■ CONCLUSIONS

We describe the development of highly active and selective heterogeneous Zn-based catalysts (3.01 kg/g-cat, f_{CO_2} = 0.97, and selectivity 91%) for the copolymerization of CO_2 and PO, resulting in the synthesis of a high molecular weight copolymer. The catalyst features extremely thin sheets composed of zinc ions, hydroxides, and gallic acid. The increased number of active sites of ultrathin sheets rendered the efficient and selective polymerization of PO and CO_2. The use of cheap zinc salts and naturally abundant gallic acid as precursors for the Zn-gallate catalyst provides nontoxic and economic advantages, which could pave the way for the commercialization of CO_2-derived polymer and ultimately contribute to achieving carbon neutrality in chemical industries.

■ ASSOCIATED CONTENT

ⓢ Supporting Information

The Supporting Information is available free of charge at https://pubs.acs.org/doi/10.1021/acssuschemeng.3c06058.

Experimental procedures of the synthesis of catalysts and polymerization reactions, analysis of polycarbonates, and additional characterization data of Zn-gallate **1** (PDF)

■ AUTHOR INFORMATION

Corresponding Authors

Seung-Joo Kim − *Department of Chemistry, Ajou University, Suwon 16499, Korea;* ◉ orcid.org/0000-0002-9945-5181; Email: sjookim@ajou.ac.kr

Hye-Young Jang − *Department of Energy Systems Research, Ajou University, Suwon 16499, Korea;* ◉ orcid.org/0000-0003-4471-2328; Email: hyjang2@ajou.ac.kr

Authors

Yongmoon Yang − *Department of Energy Systems Research, Ajou University, Suwon 16499, Korea*

Kihyuk Sung − *Department of Energy Systems Research, Ajou University, Suwon 16499, Korea*

Jong Doo Lee − *Department of Chemistry, Ajou University, Suwon 16499, Korea*

Junho Ha − *Department of Energy Systems Research, Ajou University, Suwon 16499, Korea*

Heeyoun Kim − *Department of Energy Systems Research, Ajou University, Suwon 16499, Korea*

Jinsu Baek − *Department of Chemistry, Yonsei University, Seoul 03722, Korea;* ◉ orcid.org/0000-0002-6393-9176

Jeong Hwa Seo − *Department of Chemistry, Ajou University, Suwon 16499, Korea*

Bun Yeoul Lee − *Department of Molecular Science and Technology, Ajou University, Suwon 16499, Korea;* ◉ orcid.org/0000-0002-1491-6103

Seung Uk Son − *Department of Chemistry, Ajou University, Suwon 16499, Korea;* ◉ orcid.org/0000-0002-4779-9302

Byeong-Su Kim − *Department of Chemistry, Yonsei University, Seoul 03722, Korea;* ◉ orcid.org/0000-0002-6419-3054

Yongsun Kim − *Department of Energy Systems Research, Ajou University, Suwon 16499, Korea*

Ji-Yong Park − *Department of Energy Systems Research, Ajou University, Suwon 16499, Korea;* ◉ orcid.org/0000-0001-5117-3532

Complete contact information is available at:
https://pubs.acs.org/10.1021/acssuschemeng.3c06058

Author Contributions
#Y.Y. and K.S. contributed equally to this work.

Notes
The authors declare no competing financial interest.

■ ACKNOWLEDGMENTS

■ ABBREVIATIONS

Zn:zinc; PO:propylene oxide; FE-SEM:field emission scanning electron microscopy; TEM:transmission electron microscopy; BET:Brunauer−Emmett−Teller; AFM:Atomic Force Microscopy; PXRD:powder X-ray diffraction; ICP-AES:inductively coupled plasma-atomic emission spectroscopy; IR:infrared absorption; TGA:thermal gravimetric analysis; XPS:X-ray photoelectron spectroscopy; TGA:thermogravimetric analysis

■ REFERENCES

(1) Dowell, N. M.; Fennell, P. S.; Shah, N.; Maitland, G. The role of CO_2 capture and utilization in mitigating climate change. *Nature Clim. Change* **2017**, 7, 243−249, DOI: 10.1038/nclimate3231.

(2) United Nations Environment Programme. Emissions Gap Report 2022. https://www.unep.org/resources/emissions-gap-report-2022 (accessed March 12, 2023).

(3) Burkart, M. D.; Hazari, N.; Tway, C. L.; Zeitler, E. L. Opportunities and challenges for catalysis in carbon dioxide utilization. *ACS Catal.* **2019**, 9, 7937−7956.

(4) Kamkeng, A. D. N.; Wang, M.; Hu, J.; Du, W.; Qian, F. Transformation technologies for CO_2 utilisation: Current status, challenges and future prospects. *Chem. Eng. J.* **2021**, 409, No. 128138.

(5) Quadrelli, E. A.; Centi, G.; Duplan, J.-L.; Perathoner, S. Carbon dioxide recycling: emerging large-scale technologies with industrial potential. *ChemSusChem* **2011**, 4, 1194−1215.

(6) Peters, M.; Köhler, B.; Kuckshinrichs, W.; Leitner, W.; Markewitz, P.; Müller, T. E. Chemical technologies for exploiting and recycling carbon dioxide into the value chain. *ChemSusChem* **2011**, 4, 1216−1240.

(7) Scharfenberg, M.; Hilf, J.; Frey, H. Functional polycarbonates from carbon dioxide and tailored epoxide monomers: degradable materials and their application potential. *Adv. Funct. Mater.* **2018**, 28, No. 1704302, DOI: 10.1002/adfm.201704302.

(8) Grignard, B.; Gennen, S.; Jérôme, C.; Kleij, A. W.; Detrembleur, C. Advances in the use of CO_2 as a renewable feedstock for the synthesis of polymers. *Chem. Soc. Rev.* **2019**, 48, 4466−4514.

(9) Langanke, J.; Wolf, A.; Hofmann, J.; Böhm, K.; Subhani, M. A.; Müller, T. E.; Leitner, W.; Gürtler, C. Carbon dioxide (CO_2) as sustainable feedstock for polyurethane production. *Green Chem.* **2014**, 16, 1865−1870.

(10) Inoue, S.; Koinuma, H.; Tsuruta, T. Copolymerization of carbon dioxide and epoxide with organometallic compounds. *Makromol. Chem.* **1969**, 130, 210−220.

(11) Coates, G. W.; Moore, D. R. Discrete metal-based catalysts for the copolymerization of CO_2 and epoxides: discovery, reactivity, optimization, and mechanism. *Angew. Chem., Int. Ed.* **2004**, 43, 6618−6639.

(12) Darensbourg, D. J. Making plastics from carbon dioxide: salen metal complexes as catalysts for the production of polycarbonates from epoxides and CO_2. *Chem. Rev.* **2007**, 107, 2388−2410.

(13) Sugimoto, H.; Inoue, S. Copolymerization of carbon dioxide and epoxide. *J. Polym. Sci., Part A: Polym. Chem.* **2004**, 42, 5561−5573.

(14) Kamphuis, A.; Picchioni, F.; Pescarmona, P. P. CO_2-fixation into cyclic and polymeric carbonates: principles and applications. *Green Chem.* **2019**, 21, 406−448.

(15) Grefe, L.; Mejía, E. Earth-abundant bimetallic and multimetallic catalysts for epoxide/CO_2 ring-opening copolymerization. *Tetrahedron* **2021**, 98, 132433−132448.

(16) Darensbourg, D. J.; Stafford, N. W.; Katsurao, T. Supercritical carbon dioxide as solvent for the copolymerization of carbon dioxide and propylene oxide using a heterogeneous zinc carboxylate catalyst. *J. Mol. Catal. A: Chem.* **1995**, 104, L1−L4.

(17) Lidston, C. A.; Severson, S. M.; Abel, B. A.; Coates, G. W. Multifunctional catalysts for ring-opening copolymerizations. *ACS Catal.* **2022**, 12, 11037−11070.

(18) Ree, M.; Bae, J. Y.; Jung, J. H.; Shin, T. J. A green copolymerization of carbon dioxide and propylene oxide. *Korea Polym. J.* **1999**, 7, 333–349.

(19) Ree, M.; Bae, J. Y.; Jung, J. H.; Shin, T. J. A new copolymerization process leading to poly(propylene carbonate) with a highly enhanced yield from carbon dioxide and propylene oxide. *J. Polym. Sci., Polym. Chem.* **1999**, 37, 1863–1876.

(20) Kim, J. S.; Kim, H.; Yoon, J.; Heo, K.; Ree, M. Synthesis of zinc glutarates with various morphologies using an amphiphilic template and their catalytic activities in the copolymerization of carbon dioxide and propylene oxide. *J. Polym. Sci., Polym. Chem.* **2005**, 43, 4079–4088.

(21) Ree, M.; Hwang, Y.; Kim, J.-S.; Kim, H.; Kim, G.; Kim, H. New findings in the catalytic activity of zinc glutarate and its application in the chemical fixation of CO_2 into polycarbonates and their derivatives. *Catal. Today* **2006**, 115, 134–145.

(22) Li, X.; Meng, L.; Zhang, Y.; Qin, Z.; Meng, L.; Li, C.; Liu, M. Research and application of polypropylene carbonate composite materials: a review. *Polymers* **2022**, 14, 2159.

(23) Meng, Y. Z.; Du, L. C.; Tiong, S. C.; Zhu, Q.; Hay, A. S. Effects of the structure and morphology of zinc glutarate on the fixation of carbon dioxide into polymer. *J. Polym. Sci., Part A: Polym. Chem.* **2002**, 40, 3579–3591.

(24) Padmanaban, S.; Kim, M.; Yoon, S. Acid-mediated surface etching of a nano-sized metal-organic framework for improved reactivity in the fixation of CO_2 into polymers. *J. Ind. Eng. Chem.* **2019**, 71, 336–344.

(25) Eberhardt, R.; Allmendinger, M.; Zintl, M.; Troll, C.; Luinstra, G.; Rieger, B. New zinc dicarboxylate catalysts for the CO_2/propylene oxide copolymerization reaction: activity enhancement through Zn(II)-ethylsulfinate initiating groups. *Macromol. Chem. Phys.* **2004**, 205, 42–47.

(26) Padmanaban, S.; Yoon, S. Surface modification of a MOF-based catalyst with Lewis metal salts for improved catalytic activity in the fixation of CO_2 into polymers. *Catalysts* **2019**, 9, 892–902.

(27) Chisholm, M. H.; Navarro-Llobet, D.; Zhou, Z. Poly(propylene carbonate). 1. More about poly(propylene carbonate) formed from the copolymerization of propylene oxide and carbon dioxide employing a zinc glutarate catalyst. *Macromolecules* **2002**, 35, 6494–6504, DOI: 10.1021/ma020348+.

(28) Klaus, S.; Lehenmeier, M. W.; Herdtweck, E.; Deglmann, P.; Ott, A. K.; Rieger, B. Mechanistic insights into heterogeneous zinc dicarboxylates and theoretical considerations for CO_2-epoxide copolymerization. *J. Am. Chem. Soc.* **2011**, 133, 13151–13161.

(29) Yang, Y.; Lee, J. D.; Seo, Y. H.; Chae, J.-H.; Bang, S.; Cheong, Y.-J.; Lee, B. Y.; Lee, I.-H.; Son, S. U.; Jang, H.-Y. Surface activated zinc-glutarate for the copolymerization of CO_2 and epoxides. *Dalton Trans.* **2022**, 51, 16620–16627.

(30) Kuran, W.; Rokicki, A.; Pasynkiewicz, S. On the products of reactions of zinc dialkyls with pyrogallol. *J. Organomet. Chem.* **1978**, 157, 135–143, DOI: 10.1016/S0022-328X(00)92281-2.

(31) Hussein, M. Z. b.; Ghotbi, M. Y.; Yahaya, A. H.; Rahman, M. Z. A. Synthesis and characterization of (zinc-layered-gallate) nanohybrid using structural memory effect. *Mater. Chem. Phys.* **2009**, 113, 491–496, DOI: 10.1016/j.matchemphys.2008.07.127.

(32) Ghotbi, M. Y.; Hussein, M. Z.; Yahaya, A. H.; Rahman, M. Z. Thermal decomposition pathway of undoped and doped zinc layered gallate nanohybrid with Fe^{3+}, Co^{2+} and Ni^{2+} to produce mesoporous and high pore volume carbon material. *Solid State Sci.* **2009**, 11, 2125–2132, DOI: 10.1016/j.solidstatesciences.2009.08.013.

(33) Zheng, Y.; Niu, H.; He, D.; Wang, S.; Cai, Y.; Zhang, S. Hierarchical mesoporous carbon nanosheets for efficient organic pollutants removal. *Microporous Mesoporous Mater.* **2019**, 276, 251–259.

(34) Motloung, D. M.; Mashele, S. S.; Matowane, G. R.; Swain, S. S.; Bonnet, S. L.; Noreljaleel, A. E. M.; Oyedemi, S. O.; Chukwuma, C. I. Synthesis, characterization, antidiabetic and antioxidative evaluation of a novel Zn(II)-gallic acid complex with multifacet activity. *J. Pharm. Pharmacol.* **2020**, 72, 1412–1426.

(35) Yan, Y.; Liu, Z.; Xie, P.; Huang, S.; Chen, J.; Caddeo, F.; Liu, X.; Huang, Q.; Jin, M.; Shui, L. Selective electrochemical assay of acetaminophen based on 3D-hierarchical mesoporous carbon nanosheets. *J. Colloid Interface Sci.* **2023**, 634, 509–520.

(36) Ruiz, C. V.; Rodríguez-Castellón, E.; Giraldo, O. Hybrid materials based on a layered zinc hydroxide solid and gallic acid: Structural characterization and evaluation of the controlled release behavior as a function of the gallic acid content. *Appl. Clay Sci.* **2019**, 181, No. 105228.

(37) Liao, J.-H.; Lee, T.-J.; Su, C.-T. Synthesis and characterization of a porous coordination polymer, $Zn_5(OH)_4(BDC)_3\cdot2DMF$ (DMF = *N,N*-dimethylformamide). *Inorg. Chem. Commun.* **2006**, 9, 201–204.

(38) Holden, D. L.; Goulding, H. V.; Bacsa, J.; Berry, N. G.; Greeves, N.; Stephenson, R. A.; Harrington, R. W.; Clegg, W.; Fogg, A. M. Unusual hybrid materials prepared by the oxidation of a ketone. *Cryst. Growth. Des.* **2011**, 11, 3013–3019.

(39) Shin, M.; Park, E.; Lee, H. Plant-inspired pyrogallol-containing functional materials. *Adv. Funct. Mater.* **2019**, 29, No. 1903022, DOI: 10.1002/adfm.201903022.

(40) Combs, G.; Hinney, H. R.; Bowman, P. T. Process for making double metal cyanide catalysts. US5,783,513.1998.

(41) Kong, X.; Jin, L.; Wei, M.; Duan, X. Antioxidant drugs intercalated into layered double hydroxide: structure and in vitro release. *Appl. Clay Sci.* **2010**, 49, 324–329.

(42) Kongshaug, K. O.; Fjellvåg, H. Organically pillared layered zinc hydroxides. *J. Solid State Chem.* **2004**, 177, 1852–1857.

(43) Carton, A.; Abelouhab, S.; Renaudin, G.; Rabu, P.; Francois, M. Structure of zinc hydroxy-terephthalate: $Zn_3(OH)_4(C_8H_4O_4)$. *Sold State Sci.* **2006**, 8, 958–963, DOI: 10.1016/J.SOLIDSTATESCIENCES.2006.02.043.

(44) Altomare, A.; Cuocci, C.; Giacovazzo, C.; Moliterni, A.; Rizzi, R.; Corriero, N.; Falcicchio, A. EXPO2013: a kit of tools for phasing crystal structures from powder data. *J. Appl. Crystallogr.* **2013**, 46, 1231–1235.

(45) Said, S. A.; Roberts, C. S.; Lee, J. K.; Shaffer, M. S. P.; Williams, C. K. Direct organometallic synthesis of carboxylate intercalated layered zinc hydroxides for fully exfoliated functional nanosheets. *Adv. Funct. Mater.* **2021**, 31, No. 2102631, DOI: 10.1002/adfm.202102631.